Materials Advances

ROYAL SOCIETY OF CHEMISTRY

PAPER

View Article Online
View Journal

Cite this: DOI: 10.1039/d6ma00037a

On-demand dopamine receptor activation *via* photoresponsive nanoparticle-dopamine conjugates in differentiated SH-SY5Y and transfected HEK293 cells

Hajar Alghamdi,[ab] Sunil Rajput,[b] Noah A. Russell,[c] Shailesh N. Mistry,[b] Charles A. Laughton,[b] Giuseppe Mantovani,[b] Pavel Gershkovich,[b] Keith Spriggs[b] and Mischa Zelzer *[b]

Parkinson's disease is a complex neurodegenerative disease associated with the reduction of dopamine content in the brain. Dopamine, in the form of the precursor L-DOPA, is used as a replacement therapy, which provides temporary symptomatic relief. Long-term treatment with L-DOPA induces side effects such as involuntary movements (dyskinesia) due to the continuous and non-discriminatory exposure to dopamine. Here, we propose that a reduction in the dose and frequency of administration of L-DOPA might reduce such side effects. We hypothesise that by binding dopamine to a nanoparticle *via* a photoresponsive moiety, we can not only maintain dopamine's biological activity, but also modulate the availability of dopamine for receptor activation non-invasively through light. To test this hypothesis, we designed a nanoparticle surface functionalised with a photoresponsive spiropyran molecule that is conjugated to dopamine to stimulate activation of the dopamine D_1 receptor (D_1R). The activity of the system was assessed using a cAMP assay on a Parkinson's disease modelled SH-SY5Y neuroblastoma cell line and DRD1/CRE transfected HEK293 cells. We found that cAMP concentration was elevated in treated cells, meaning that the biological activity of conjugated dopamine is maintained and that the dopaminergic receptor is activated on-demand by light stimulation in our model system.

Received 7th January 2026,
Accepted 29th April 2026

DOI: 10.1039/d6ma00037a

rsc.li/materials-advances

Introduction

Parkinson's disease (PD) is a complex neurodegenerative disease associated with a reduction of dopamine in the nigrostriatal pathway alongside the degeneration of dopaminergic neurons in the substantia nigra (SN) brain region.[1] It is the second most common neurodegenerative disease with a cumulative global prevalence of 23.6%[2] and an anticipated increase in prevalence from 2021 to 2050 of 76%.[3] The annual socio-economic cost of PD is estimated at €250 billion.[4]

PD is currently treated by dopamine replacement therapy that provides temporary symptomatic relief.[5] While several treatment modalities can be considered,[5] administration of levodopa (L-DOPA) is the prevalent choice due to its greater symptomatic efficacy compared to other dopamine agonists.[5,6] However, L-DOPA induces involuntary movements, dyskinesia, which occur in more than half of PD patients after 5–10 years of treatment. In addition, nearly 40% of patients experience motor fluctuations after 4–6 years of using L-DOPA.[6] To delay the onset of adverse effects caused by L-DOPA treatment, combined administration of dopamine D_1 receptor (D_1R) agonists and L-DOPA is suggested to directly activate the D_1R and bypass the presynaptic synthesis of dopamine;[7,8] however, at present this approach is hampered by the lack of a non-invasive, safe, long-term treatment modality to activate D_1R.

Delivery systems activated using light-responsive molecules are promising tools for manipulating the activity of dopamine receptors.[9,10] These systems hold potential for clinical applications due to improved control over the therapeutic effect and the ability to account for inter-patient variability.[11] For example, light-responsive dopamine receptors (DARs) were designed wherein the receptor ligand is covalently bound to the receptor *via* an azobenzene linker.[12,13] The ligand's availability to the receptor is controlled by light-induced *cis–trans* isomerisation of the azobenzene linker. This approach requires genetic engineering to introduce a chemical attachment site for the azobenzene-linked dopamine on the receptor; it therefore cannot be readily administered as a therapeutic. Light-induced

[a] School of Pharmacy, University of Hafr Albatin, Hafr Albatin, Kingdom of Saudi Arabia
[b] School of Pharmacy, University of Nottingham, University Park, Nottingham, NG7 2RD, UK. E-mail: mischa.zelzer@nottingham.ac.uk
[c] University of Nottingham, University Park, Nottingham, NG7 2RD, UK

release of caged DAR antagonists has been reported, which provides the means for non-reversible stimulation of DARs.[14] A recent example for reversible DAR stimulation is azodopa, a photoresponsive compound that was shown to reversibly control dopamine receptor activity in anesthetized mice and increase neural activity in the cortex.[15] A notable disadvantage of azodopa is that it remains in its biologically active, thermodynamically stable *trans*-state unless continuously exposed to UV light (λ = 365 nm) to maintain its biologically less active *cis*-state.

The aim of our work is to develop a system that can reversibly activate D_1R in response to light on-demand, but remains inactive in the absence of a photostimulus. In contrast to the azobenzene/dopamine derivatives used previously (*e.g.*, to develop azodopa[15]), spiropyran is a photo-responsive compound whose thermodynamically more stable form is its closed state.[16] The open merocyanine form of spiropyran is less prevalent but does exist in an equilibrium with the closed spiropyran form. This equilibrium is predominantly shifted towards the closed spiropyran form if the system is in thermodynamic equilibrium or if it is irradiated with visible light. The prevalence of the two isomers can be shifted towards the open merocyanine form upon irradiation with UV light at λ = 365 nm.[17] Here, we propose that if a ligand such as dopamine is attached to spiropyran, the bulkiness of the closed spiropyran form would prevent or reduce fitting of the ligand into the binding pocket of its receptor. The light-induced change to the open merocyanine form would reduce this steric hindrance and increase the fit of the conjugated ligand to the receptor binding site. We designed and synthesised a conjugated photo-responsive system from spiropyran and dopamine, immobilised on silica nanoparticles, and demonstrated that this system can stimulate D_1R upon external light stimulation but remains inactive in the absence of a photo-stimulus (Fig. 1).

Results and discussion

The proposed light-responsive dopamine receptor stimulation system consists of dopamine, which is immobilised on a silica-nanoparticle (SiNP) with a photo-responsive spiropyran linker (Fig. 1). This required (i) fabrication of nanoparticles; (ii) synthesis of a difunctional spiropyran-based linker; and (iii) functionalisation of silica nanoparticles with the spiropyran linker followed by conjugation of dopamine to the linker.

Design and synthesis of the spiropyran linker

The photoresponsive linker (**7**) is based on spiropyran and was synthesised as shown in Fig. 2A. Precursor **4** was synthesised by treatment of 3-(chloromethyl)-2-hydroxy-5-nitrobenzaldehyde with sodium azide in DMSO. In parallel, 4-hydrazinobenzoic acid and 2-methyl-2-butanone were reacted in ethanol using H_2SO_4 as the acid catalyst to give 2,3,3-trimethyl-3*H*-indole-5-carboxylic acid (**5**), which was then treated with methyl iodide to give 5-carboxy-1,2,3,3-tetramethyl-3*H*-indol-1-ium iodide (**6**).[17,18] Finally, the spiropyran (SP) linker (**7**) was obtained from **4** and **6** under microwave irradiation. The chemical identity of all compounds was confirmed by NMR and mass spectrometry (Section S1 and Fig. S1–S4, SI).

Spectroscopic characterisation of spiropyran derivative 7

Fluorescence spectroscopy was used to characterise the photoresponsive behaviour of spiropyran derivative **7**. It has previously been observed that spiropyran derivatives experience solvatochromism and that their ability to undergo photoresponsive conformational changes depends on the solvent system used.[19] Similar to previously reported observations,[19] we found that compound **7** shows no change in its fluorescence spectrum upon exposure to UV light at 365 nm when dissolved in water (data not shown). Conversely, in a 1 : 1 water : acetonitrile solution, UV-induced conversion from the cyclic spiropyran to the open merocyanine form was observed. Accordingly, after irradiation at 365 nm, the fluorescence emission intensity around 460 nm (λ_{Ex} = 350 nm, associated with the SP form) decreased (Fig. 2B) while the fluorescence emission intensity around 650 nm (λ_{Ex} = 550 nm, associated with the merocyanine form[18]) increased (Fig. 2C). Because the subsequent *in vitro* application studies were conducted in cell culture medium, we also measured the fluorescence emission in indicator-free neurobasal medium.

No fluorescence emission for compound **7** was observed from the SP form (λ_{Ex} = 350 nm) in indicator-free neurobasal media, regardless of the sample conditioning (data not shown). When excited at λ_{Ex} = 550 nm, fluorescence emission peaks between 600 nm and 700 nm, typically associated with the merocyanine form,[18] can be observed (Fig. 2D). If pre-conditioned with visible light, this emission is very weak (Fig. 2D, yellow spectrum). After exposing the solution of compound **7** to 365 nm for 30 min, a more intense fluorescence emission peak around 640 nm characteristic of the open merocyanine form is observed (Fig. 2D, red spectrum). These data demonstrate that spiropyran derivative **7** undergoes photoresponsive conformational changes in neurobasal media and can thus be used in the *in vitro* study of the photoresponsive receptor activation system.

Nanoparticle synthesis

Silica nanoparticles (SiNPs) are prepared *via* the Stöber method and characterised by DLS and TEM. The mean hydrodynamic diameter of the particles obtained by DLS is 45.9 ± 0.4 nm and the polydispersity index (PDI) is 0.12 ± 0.01 (Fig. S5A, SI). TEM shows that the SiNPs are spherical (Fig. S5B, SI), and that the population appears homogenous in size, with no aggregates observed. The mean particle diameter determined by TEM is 33 ± 0.9 nm. The smaller size measured by TEM compared to DLS is consistent with the different measurement principles (dry particle diameter *vs.* hydrodynamic diameter) of these two techniques.

Nanoparticle modification

To prepare the SiNPs for the conjugation of compound **7** through copper(I)-catalyzed alkyne–azide cycloaddition (CuAAC) (Fig. 3A), alkyne groups were introduced on the surface of the SiNPs by silanisation of the SiNPs with 3-(aminopropyl)trimethoxysilane to yield amine functionalised particles (SiNP–NH_2), followed by

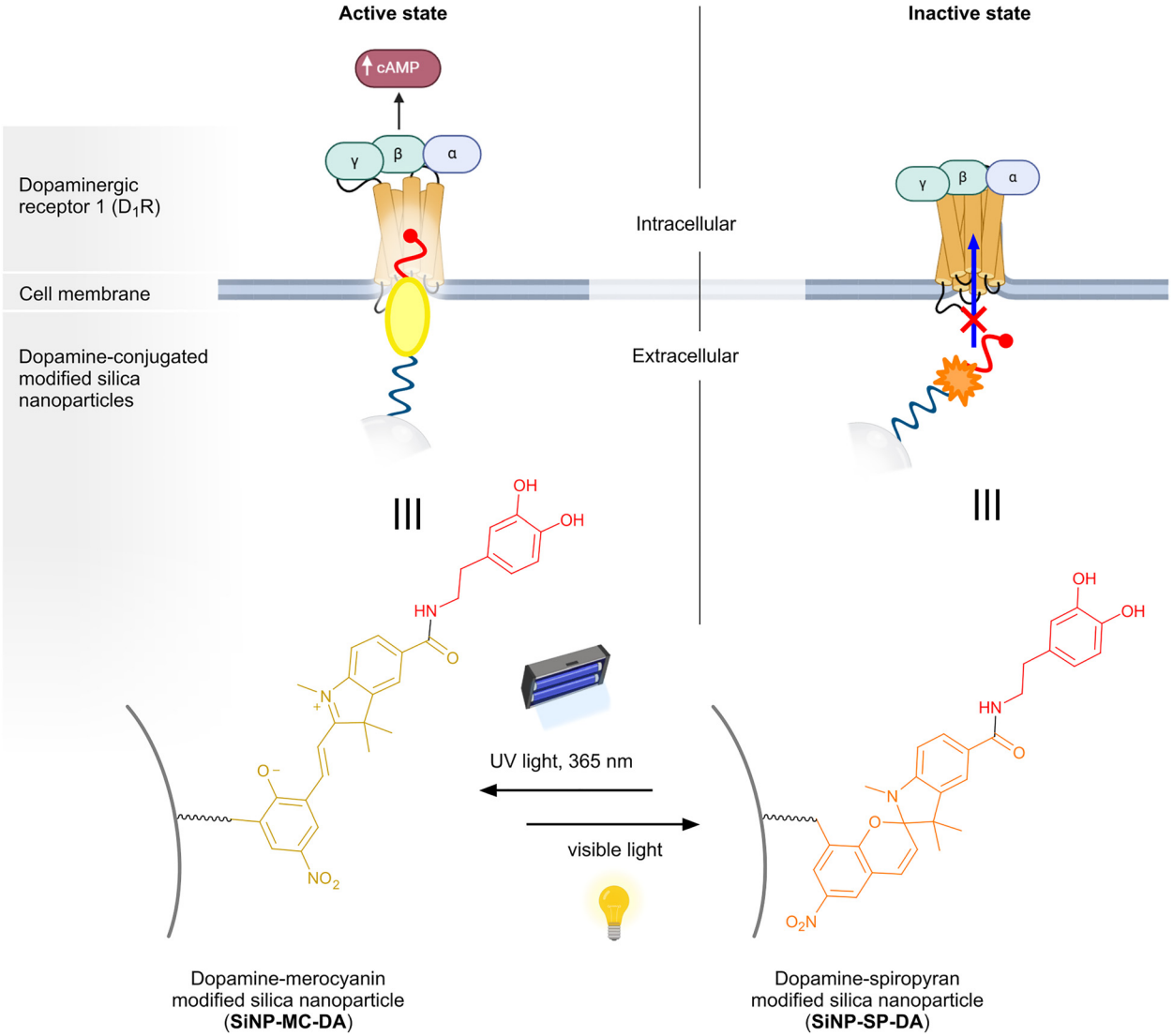

Fig. 1 Conceptual representation of the on-demand activation of D_1R with silica nanoparticles (SiNPs) modified with a light-responsive dopamine–spiropyran conjugate. Spiropyran (SP) predominantly remains in its closed form under visible light (and in the dark), preventing the conjugated dopamine from effectively interacting with D_1R. Upon exposure to UV light at λ = 365 nm, spiropyran adopts its open form (merocyanine, MC), which enables the conjugated dopamine (DA) to interact with and stimulate D_1R. Partly created in BioRender. Alghamdi, H. (2026) https://BioRender.com/16zd09k.

reaction with pentynoic acid (SiNP–Alkyne) (Fig. S6, SI). SiNP–Alkyne particles can then be reacted with 7 to introduce spiropyran to the surface of the nanoparticles (SiNP–SP). In the last step, dopamine is conjugated to these spiropyran groups *via* carbodiimide-mediated amide bond formation (SiNP–SP–DA) (Fig. 3A).

As a control for the *in vitro* study below, dopamine functionalised SiNPs without spiropyran (SiNP–DA) were prepared by reacting succinic anhydride with SiNP–NH_2 particles to introduce COOH functionalities (SiNP–COOH) to which dopamine was then grafted (Fig. S7, SI).

The particle surface modification steps are followed by zeta potential measurements (Fig. 3B and Fig. S8, SI). Attachment of 3-(aminopropyl)trimethoxysilane (APTMS) to create amine-terminated surfaces results in a change of the particle surface charge from negative to positive. This is consistent with previously published work.[20,21] When reacted with 4-pentynoic acid to create alkyne terminated surfaces followed by attachment of spiropyran and dopamine, the particles maintain their positive zeta potential. This contrasts with the expectation that COOH groups (in spiropyran) and OH groups (in dopamine) are likely to introduce negative charges on the particle surface but can be explained if functionalisation is incomplete. The degree of functionalisation was not investigated in detail here; thus, to maintain consistency and comparability within this study, all subsequent biological functionality tests were conducted with the same batch.

Preparation of the SiNP–COOH from SiNP–NH_2 results in a negative zeta potential due to the COOH functionalities (Fig. S8, SI). Subsequent attachment of dopamine to form SiNP–DA renders the particle charge positive again.

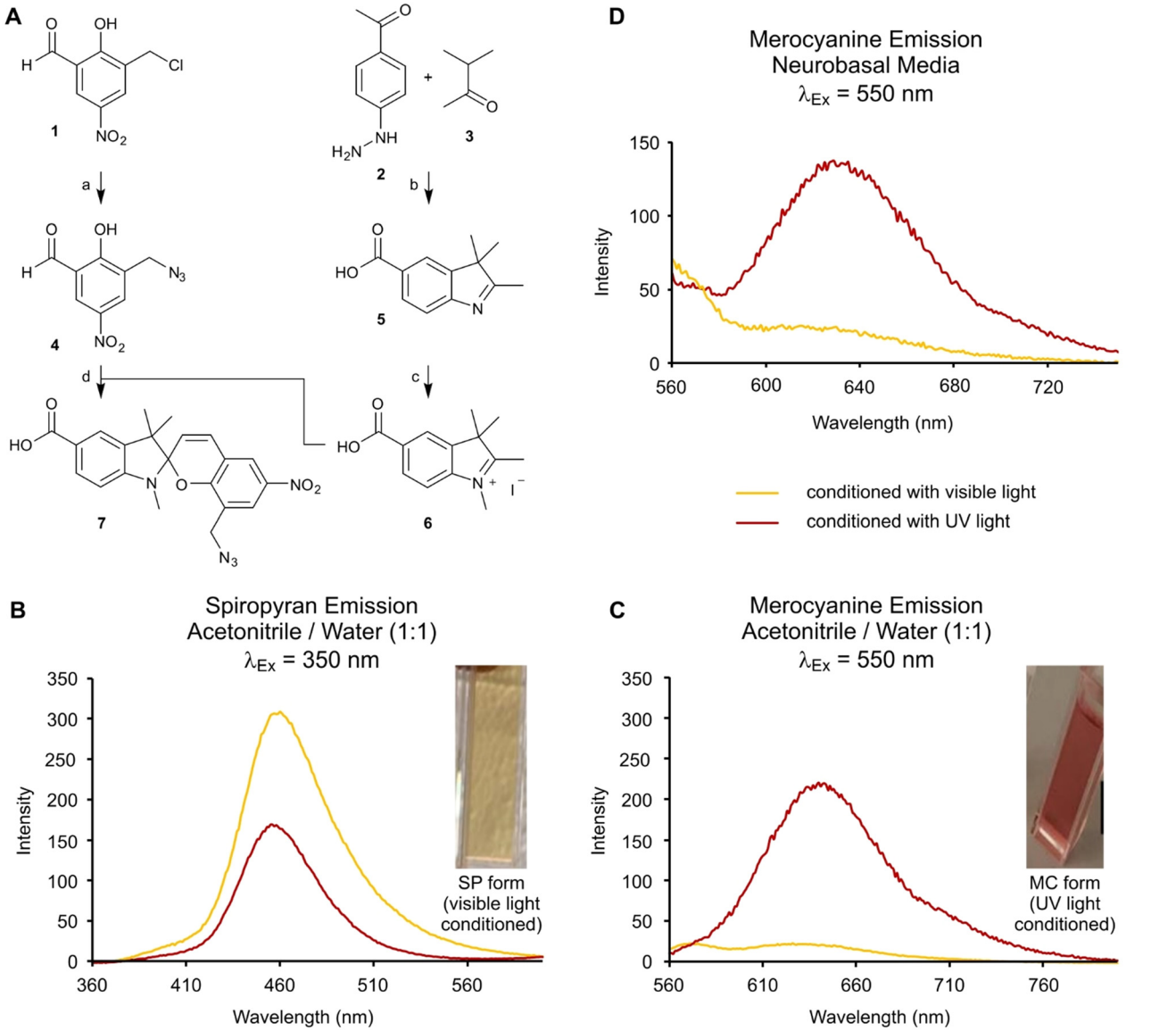

Fig. 2 Synthesis and spectroscopic characterisation of the spiropyran-based photoresponsive linker **7**. (A) Reaction schematic for the synthesis of 8-(azidomethyl)-1′,3′,3′-trimethyl-6-nitrospiro[chromene-2,2′-indoline]-5′-carboxylic acid (**4**). Reaction conditions: (a) NaN_3, DMSO, N_2, rt, 18 h; (b) H_2SO_4 (cat), ethanol, N_2, reflux, 18 h; (c) CH_3I, toluene/acetonitrile, 95 °C, 24 h; (d) Et_3N, acetonitrile, microwaves at 40 °C and 250 W, 10 min. (B)–(D) Fluorescence emission spectra of spiropyran derivative **4** in acetonitrile : water (1 : 1) (B) and (C) and indicator-free neurobasal culture media (D) obtained at λ_{Ex} = 350 nm ((B), indicative of the spiropyran form) and λ_{Ex} = 550 nm ((C) and (D), indicative of the merocyanine form) after exposure to daylight for 5 minutes (yellow) (preconditioned to drive the equilibrium to the spiropyran form) or exposure to UV light (365 nm) for 30 minutes (red) (preconditioned to drive the equilibrium to the merocyanine form). Inset images show the optical appearance of preconditioned samples in acetonitrile/water (1 : 1). No spiropyran signal at λ_{Ex} = 350 nm was observed for either preconditioned sample.

The SiNP surface modification is also confirmed with FTIR (Fig. 3C and Fig. S9, SI). The IR spectra interpretation is summarised here; for detailed peak assignments please refer to Section S3 (SI).

Unmodified SiNPs show typical peaks for silica. The introduction of amine groups (modification of SiNP with APTMS to yield SiNP–NH_2) is confirmed by the appearance of aliphatic signals and peaks that can be assigned to protonated amines (NH_3^+). The conversion of SiNP–NH_2 to SiNP–Alkyne *via* amide bond formation between the amines and pentynoic acid is supported by a strong C═O peak at 1648 cm^{-1} indicative of amides and a strong reduction of the amine peak at 1547 cm^{-1} compared to SiNP–NH_2. Subsequent addition of SP to form SiNP–SP shows signals from the COOH and NO_2 groups as well as a signal for a cyclic ether of the SP derivative. These assignments are in line with previous observations on spiropyran conjugated to carbon nanoparticles.[22] The absence of a signal around 2100 cm^{-1} for the stretch vibration of the azide further supports successful conjugation of SP to the particles *via* CuAAC. It should be noted that the peak positions of SP are known to change when transitioning to the MC form,[23] and that the data shown here likely represents a mixture of the SP and MC forms.

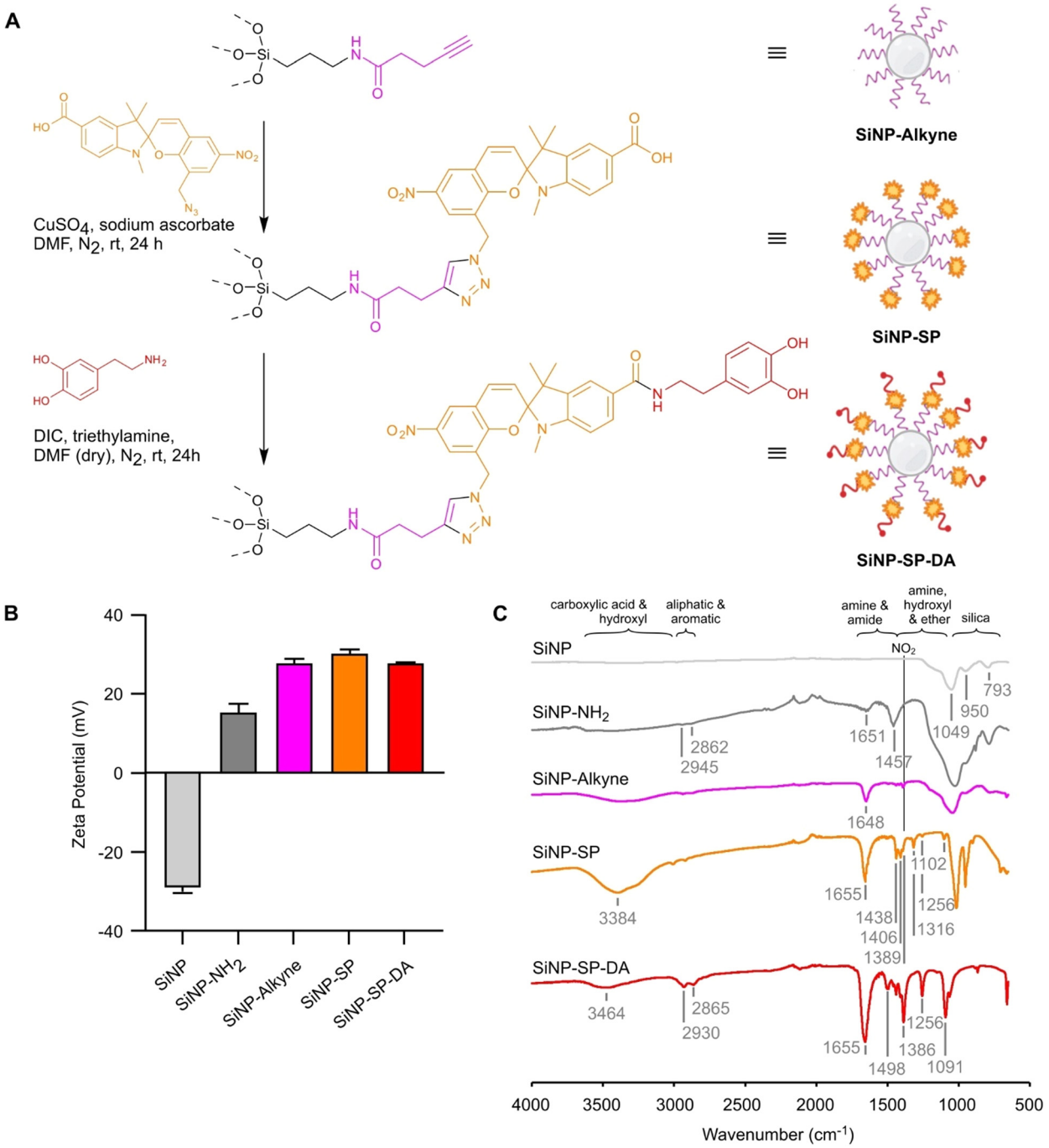

Fig. 3 Preparation and characterisation of silica nanoparticles modified with the dopamine–spiropyran conjugate (SiNP–SP–DA). (A) Surface modification steps to prepare SiNP–SP–DA. Silica nanoparticles functionalised with alkyne groups (SiNP–alkyne) are reacted with 8-(azidomethyl)-1′,3′,3′-trimethyl-6-nitrospiro[chromene-2,2′-indoline]-5′-carboxylic acid (compound **7**) to yield spiropyran functionalised particles (SiNP–SP) to which dopamine is subsequently attached. (B) and (C) The surface charge and chemical functionalities were measured by zeta potential measurements (B) and infrared spectroscopy (C). The data shown include the precursor steps to make SiNP–alkyne shown in Fig. S5. (B) The zeta potential changes from negative to positive after the first SiNP modification step and remains over 20 mV, indicating good particle stability. Data represent the average of 3 measurements. Errors represent standard deviations. (C) Infrared spectra show the change in surface chemical compositions of the particles for each subsequent modification step. Partly created in BioRender. Alghamdi, H. (2026) https://BioRender.com/c3yahay.

After conversion of the COOH group to an amide bond to form SiNP–SP–DA, the intensity of the COOH peak at 3000–3600 cm^{-1} reduces while the intensity of the C═O stretching signal from the amide at 1655 cm^{-1} increases strongly. Together with a notable presence of aromatic peaks at 2930 cm^{-1} and 2865 cm^{-1} that are also present in the SiNP–DA sample (Fig. S9, SI) and have been reported before for dopamine,[24] these data suggest successful particle modification with SP–DA.

Photopharmacology of SiNP–SP–DA using SH-SY5Y cells

To test the activity and photoresponsiveness of SiNP–SP–DA, neuronal cells that contain dopaminergic receptors are required. SH-SY5Y cells are established model cells to study Parkinson's disease[25] and can be differentiated from a neuroblast-like state into a model that replicates aspects of the phenotype of mature neurons.[26] Here, we differentiate SH-SY5Y cells into mature dopaminergic neurons with retinoic acid (RA) to obtain cells that express the D_1R.[27,28]

The effect of the presence of SiNPs on the viability of SH-SY5Y cells was evaluated with an MTT cytotoxicity assay (Fig. S10A, SI). The presence of SiNPs leads to a substantial reduction in cell viability across all concentrations tested but also showed a clear concentration dependence. SiNP concentrations of 13 μg ml^{-1}, 31.25 μg ml^{-1} and 62.5 μg ml^{-1} displayed a cell viability of 62%, 55% and 53% compared to the control. At higher SiNP concentrations, cell viability dropped below 50%. This matches literature observations wherein SH-SY5Y exposed to 50 nm SiNPs at concentrations of 50 μg ml^{-1} and 100 μg ml^{-1} remained viable, even though cell viability did decrease and higher ROS production was observed in the presence of the particles.[29] As the difference in cell viability between the three lowest SiNP doses in our experiment was not substantial, a SiNP concentration of 62.5 μg ml^{-1} was chosen for subsequent photopharmacological investigations to maximise the SiNP dose while keeping cell toxicity below 50%.

The chosen SiNP dose of 62.5 μg ml^{-1} falls in a similar concentration regime as that of levodopa administered to Parkinson patients (<400 mg per day[30] with a bioavailability in the central nervous system of ~1%[31] assuming a fluid volume of ~100 ml). The exact dose of dopamine on the particles cannot be compared as the surface density of dopamine on the nanoparticle surface in our system was not determined.

To model a neurodegenerative disease state wherein the dopamine activity is reduced, differentiated SH-SY5Y (d-SH-SY5Y) cells were exposed to 1-methyl-4-phenylpyridinium (MPP+). MPP+ is a neurotoxin that has previously been used to create a model for neurodegenerative diseases which exhibits reduced dopamine receptor activity.[27,28,32]

Activation of dopamine receptors was measured with a cAMP assay (Fig. 4A). After MPP+ exposure, the cAMP activity of d-SH-SY5Y cells reduced approximately 10-fold, confirming that MPP+ treated, differentiated SH-SY5Y (MPP+-d-SH-SY5Y) cells display suitable characteristics to study the ability of dopamine-modified, light-responsive SiNPs to induce dopamine receptor activation on demand.

To determine if the dopamine immobilised on SiNP–SP–DA can interact with dopamine receptors and increase their activity, MPP+-d-SH-SY5Y cells are incubated with SiNP–SP–DA, which were pre-conditioned to adopt either the open (spiropyran, SP) form using visible light or the closed (merocyanine, MC) form, using λ = 365 nm. These two states are denoted as SiNP–SP–DA and SiNP–MC–DA, respectively. cAMP levels are measured at 30 min and 60 min, to explore potential differences in cAMP levels over a timeframe within which equilibration between the SP and MC states is likely to occur. As a control, SiNP–DA particles are used.

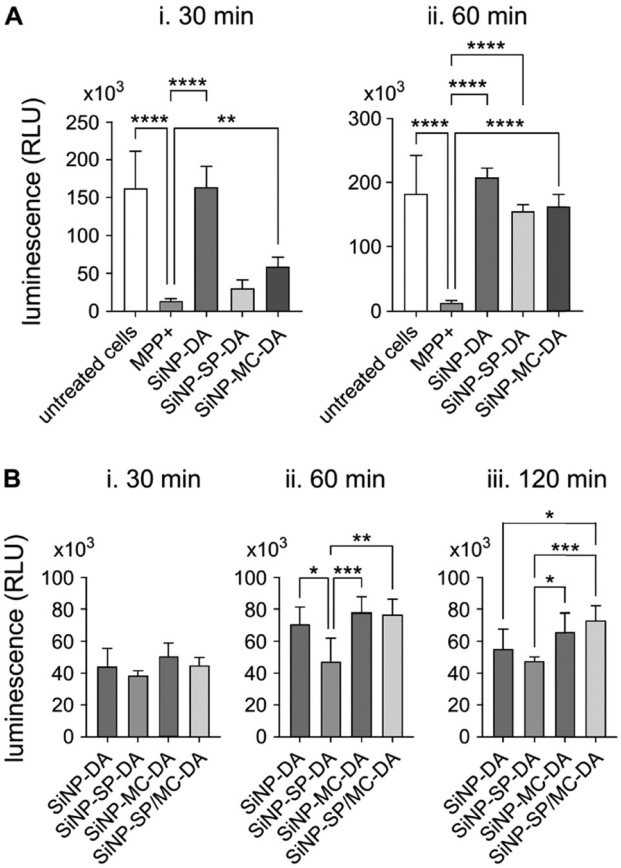

Fig. 4 Dopamine receptor activity of differentiated SH-SY5Y (A) and HEK293 (B) cells in the presence of pre-conditioned SiNP surface functionalised with the dopamine–spiropyran conjugate. (A) Dopamine receptor activity measured with a cAMP assay of MMP+-d-SH-SY5Y cells incubated with either SiNP–DA, SiNP–SP–DA or SiNP–MC–DA. Measurements were taken after 30 min (Ai.) and 60 min (Aii.) incubation with particles. MMP+-d-SH-SY5Y cells that were not exposed to SiNPs and d-SH-SY5Y cells were used as controls. (B) D_1R activity measured *via* oneGlow luciferase assay to detect luciferase luminescence in DRED1/CRE transfected HEK293 cells. Functionalised particles were used either after exposure to visible light for 30 minutes (SiNP–SP–DA) or after exposure to UV light at 365 nm for 30 minutes (SiNP–MC–DA) to drive the conformational equilibrium towards either the closed spiropyran (SP) or open merocyanine (MC) conformation. SiNP–SP/MC–DA samples were left to adopt an equilibrium of conformations by keeping them in the dark for one day. SiNP–DA particles were used as control samples. All values are reported as mean ± SD of 3 biological repeats (n = 3). Statistical significance was tested using ANOVA with a Tukey post-test. Asterisks indicate significances of ****$p < 0.001$, ***$p < 0.001$, **$p < 0.01$ and *$p < 0.05$.

Incubation of MPP+-d-SH-SY5Y cells with SiNP–DA, where dopamine is surface immobilised on a particle but not adjacent to a bulky group, increases the cAMP level to that of the d-SH-SY5Y cells for both timepoints (Fig. 4A). This suggests that dopamine retains its biological activity after surface immobilisation *via* its amine group, supporting the hypothesis that surface-immobilised dopamine remains biologically active for the activation of dopaminergic receptors.

At the 30 minute incubation timepoint, MPP+-d-SH-SY5Y cells exposed to SiNP–SP–DA show no significant increase in cAMP levels compared to MPP+ treated cells (Fig. 4Ai). In contrast, SiNP–MC–DA causes a statistically significant increase in cAMP levels, presumably due to the different conformation of the spiropyran linker in the MC compared to the SP state.

The cAMP increase obtained with SiNP–MC–DA after 30 min incubation is approximately three times lower than that obtained with SiNP–DA. At 60 min, cAMP levels for all SiNP containing experiments are not statistically significantly different from that of untreated d-SH-SY5Y cells (Fig. 3Aii). We hypothesise that the lack of a difference in cAMP levels between SiNP–SP–DA and SiNP–MC–DA might be due to the spiropyran isomerisation returning to equilibrium between 30 min and 60 min, resulting in no measurable difference between the biological activity of these two conditions. Additionally, dopamine in SiNP–MC–DA has a lower biological effect than dopamine in SiNP–DA, but dopamine receptor activity recovery to similar levels can be achieved over a longer time period. This could be explained if the sample reaches an equilibrium between the SP and the MC form within 60 min, rendering both conditions equivalent in terms of dopamine availability at that time point.

Photopharmacology of SiNP–SP–DA using HEK293 cells

While MPP+-d-SH-SY5Y cells are an established disease model for neurodegenerative diseases and exposure of these cells to SiNP–SP–DA and SiNP–MC–DA showed measurable differences in biological activity, cAMP measurements of the differentiated SH-SY5Y cell line represent the combined activity and response of all receptor types linked to cAMP generation. In addition to exploring the overall cell response, we are interested in understanding how differentially SiNP–SP–DA and SiNP–MC–DA address the activity of a single dopamine receptor type. To study this, the cAMP activity assay in the presence of modified SiNPs is performed with a dopaminergic transfected HEK293 cell line (DA-HEK293) transiently expressing the DRD1 receptor.

The cytotoxicity of unmodified SiNP on DA-HEK293 cells was measured using an MTT assay after 24 h of exposure to SiNPs at concentrations ranging from 15 μg ml^{-1} to 1000 μg ml^{-1}. At low SiNP concentrations of 15 μg ml^{-1} and 31.25 μg ml^{-1}, cell viability remained high at 85% and 79%, respectively. At 62.5 μg ml^{-1} of SiNP, cell viability was measured at 55%. Higher SiNP concentrations showed a reduction in cell viability below 50%. These observations align with literature reports showing that the HEK293 cell line displays some level of toxicity in the presence of 50 nm SiNPs at concentrations of 100 μg ml^{-1} but not at 25 μg ml^{-1}.[33,34] Based on our cytotoxicity data and for comparison with the SH-SY5Y cell data, we maintained an SiNP concentration of 62.5 μg ml^{-1} for the subsequent experiment with DA-HEK293 cells. This SiNP concentration shows similar cell viability and presents the same SiNP–DA and SiNP–SP–DA doses for both cell lines.

For the testing of the modified particles with DRD1 receptor-expressing HEK293 cells, SiNP–DA is used as a control as this is shown to provide a reasonable baseline comparison to the activity of untreated cells (Fig. S11, SI). Because the SH-SY5Y experiment indicated that conformational equilibration of spiropyran may play a role in the time-dependent response of cells, in addition to SiNP–SP–DA and SiNP–MC–DA, a third particle condition is included wherein the particles are allowed to reach conformational equilibrium by storing them in the dark before use (SiNP–SP/MC–DA).

Light exposure of the particles is performed before addition of the particles to the cells to remove the possibility of the light exposure affecting the cell response. Because isomerisation of the spiropyran has been observed to take place after 60 min in SH-SY5Y culture, the medium for the DA-HEK293 is replaced with fresh medium containing preconditioned modified SiNPs at each 30 min timepoint.

After incubation of DA-HEK293 with modified SiNPs for 30 minutes, no significant changes in cAMP levels are observed (Fig. 4Bi). Incubation for 60 minutes leads to an increase in cAMP levels for cells exposed to SiNP–DA and SiNP–MC–DA compared to the 30 min timepoint (Fig. 4Bii). The cAMP levels for SiNP–SP–DA remain at similar levels at 30 min and 60 min and are significantly lower than those of the other samples at 60 min. This suggests that the closed spiropyran form in SiNP–SP–DA reduces the biological activity of dopamine on the DRD1 receptor, whereas the activity of the open merocyanine form in SiNP–MC–DA is comparable to that of SiNP–DA.

At the 120 min incubation timepoint (Fig. 4Biii), SiNP–SP/MC–DA outperforms SiNP–DA which has returned to a cAMP level similar to that of the 30 min timepoint and is again comparable to SiNP–SP–DA after 120 min incubation. The cAMP level for SiNP–MC–DA is significantly higher than that measured for SiNP–SP–DA at 120 min. These data demonstrate that the activity of dopamine conjugated to the spiropyran SiNP can be controlled by changing the conformation of spiropyran from the closed to the open form. The cAMP levels measured in DA-HEK293 cells indicate that for the D_1R, the elevated receptor activity caused by SiNP–MC–DA increases with increasing incubation time and, after 120 min, is even more effective than SiNP–DA.

Modified SiNPs that were allowed to reach conformational equilibrium (SiNP–SP/MC–DA) showed no statistically significant difference in their cAMP level induction compared to SiNP–MC–DA. This may either mean that the MC form is prevalent in the equilibrium state under these conditions, or it could indicate that there is a threshold concentration of particles above which no additional effect is observed.

In silico docking

In the previous section, we proposed that the difference in the biological activity of SiNP–SP–DA and SiNP–MC–DA could be explained by a difference in the binding affinity of dopamine caused by the different conformation of spiropyran in its open and closed form. In its merocyanine form, the molecule's degrees of freedom increase as it has more rotatable bonds. This increased structural flexibility could lead to a better fit of dopamine in the active site of the receptor. In addition, the

charges present in merocyanine may change the binding affinity of the dopamine–merocyanine conjugate. To explore this hypothesis, docking studies were performed.

The ligands used in the docking study are dopamine conjugated to either the closed spiropyran (SP–DA) or the open merocyanine (MC–DA) form. To mimic the attachment point of the SP/MC–DA conjugates to the particle, a triazole was included in the SP/MC structures (Fig. 5A and B).

As a model dopamine receptor, D_1R (PDB ID:7CKW) was used.[35] In the docking study, unmodified dopamine is docked

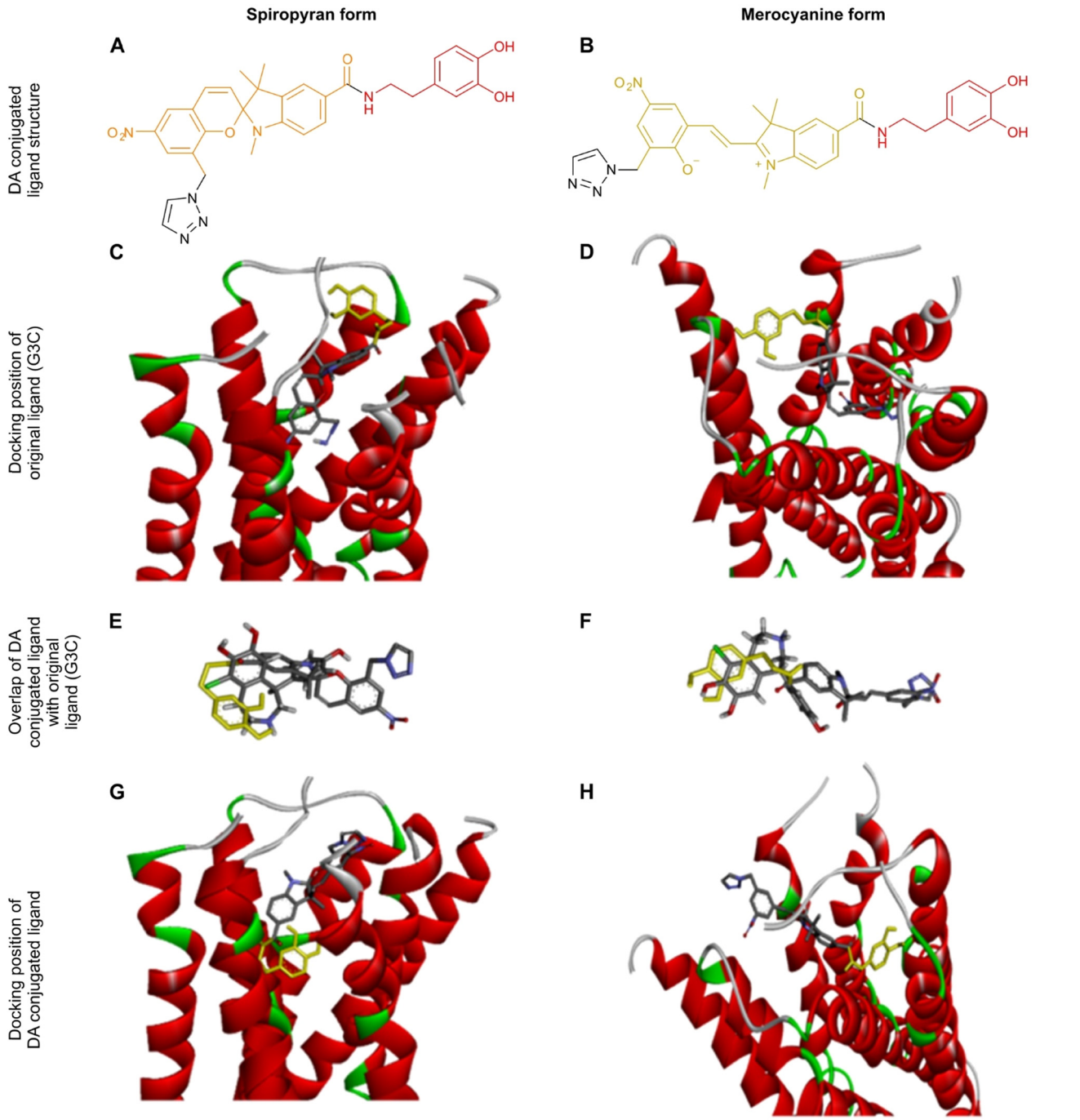

Fig. 5 Docking study of the closed (SP) and open (MC) form of the dopamine–spiropyran conjugate with the dopamine 1 receptor D1R (PDB ID:7ckw). (A) and (B) Chemical structure of the ligands used in the docking study. A triazole was included to represent the linking point to the remainder of the particle surface. (C) and (D) Docking position of the original ligand (G3C) in the crystal structure of the active site of D_1R that corresponds to the best docking score from AutoDock Vina. (E) and (F) Overlap of the dopamine (DA) conjugated spiropyran ligands with the structure of the original ligand (G3C) from the D_1R crystal structure. (G) and (H) Docking position of the DA conjugated spiropyran ligands in the active site of the D_1R receptor that corresponds to the best docking score from AutoDock Vina. The dopaime part of the molecule is shown in yellow; the SP, MC and G3C structures are shown in grey.

into D_1R first to investigate how well it fits into the binding site of the receptor. Dopamine fits well within the D_1R binding site, where it is positioned such that it overlaps closely with the co-crystallised ligand of the structure (Fig. S12, SI). The calculated binding energy of dopamine in the D_1R receptor was -6.3 kcal mol^{-1}. This provides confidence that the D_1R crystal structure is a reasonable model for the docking study of the dopamine-conjugates.

Docking of SP–DA and MC–DA to the D_1R receptor shows that both conformations fit into the receptor binding site (Fig. 5G and H). MC–DA (-10.3 kcal mol^{-1}) has a higher binding affinity than SP–DA (-6.7 kcal mol^{-1}). This supports the hypothesis that MC–DA, and by extrapolation SiNP–MC–DA, has a higher biological activity compared to the closed spiropyrane analogue due to an increased binding affinity with the active site of the dopamine receptor.

Conclusions

Light-responsive activation of treatment modalities has the potential to allow on-demand delivery of pharmacologically active stimuli or compounds. The aim of this study was to demonstrate that it is conceptually possible to non-invasively trigger activation of dopamine receptors on demand.

We successfully synthesised a new nanoparticle-based system wherein dopamine is conjugated to the particle *via* a light-responsive spiropyran unit. Using light, it is possible to change the conformation of spiropyran and thus influence the biological activity of the conjugated dopamine. In the extended merocyanine state, the conjugated dopamine was able to activate dopamine receptors in SH-SY5Y cells that were differentiated into dopaminergic neurons and in CRE/DRD1 transfected HEK293 cells. Molecular docking studies showed that the binding affinity of dopamine to the D_1R dopamine receptor is significantly higher when dopamine is conjugated to the open merocyanine form as opposed to the closed spiropyran form.

These results demonstrate that it is possible to activate dopamine receptors on demand using photoresponsive particles. For potential translation into a clinical application, several factors will have to be investigated. Firstly, the effect of the presence of nanoparticles on cell function and morphology would have to be investigated. Secondly, in addition to photo-induced isomerisation, the spiropyran/merocyanine transition can also be affected by temperature, pH changes, and solvent polarity. While we did test the system *in vitro* under physiological conditions, further investigation into the sensitivity of the system to these other factors would be needed before *in vivo* translation. The key advantage of this new light-responsive system is its ability to be activated on demand as opposed to being deactivated on demand. This allows better control over the frequency and duration of the receptor stimulation and minimises the on-time of the photostimulus. Currently, for experimental convenience, the photostimulus used is in the UV region. This is problematic for *in vivo* applications because of potential cell damage and reduced tissue penetration depth. Before *in vivo* translation, this system will have to be adapted to respond to light with higher wavelengths to improve tissue penetration and avoid damage to cells during application.

Experiments

Spiropyran synthesis

The spiropyran (SP) derivative was synthesised as shown in Fig. 2A following previously established procedures.[18]

3-Azidomethyl-2-hydroxy-5-nitrobenzaldehyde (4)[18]. 3-(Chloromethyl)-2-hydroxy-5-nitrobenzaldehyde (**1**) (500 mg, 2.3 mmol, 1 eq.) was added to a solution of sodium azide (166 mg, 2.6 mmol, 1.1 eq.) in anhydrous DMSO (4.6 ml). The mixture was stirred at room temperature under nitrogen for 18 h. H_2O (5 ml) was added dropwise, and the mixture was extracted with ethyl acetate (2×20 ml). The combined organic phase was washed with H_2O (20 ml), dried over Na_2SO_4 and concentrated under vacuum to give (**4**) as a yellow solid, which was used for the following step without further purification.

^{1}H NMR (400 MHz, DMSO-d_6): δ = 10.21 (s, CHO–(C), 1H), 8.64 (d, J = 2.9 Hz, Ar–H (C4), 1H), 8.50 (d, J = 2.9 Hz, Ar–H (C6), 1H), 4.62 (s, C8, 2H).

^{13}C NMR (400 MHz, DMSO-d_6): δ = 193.9 (C7), 163.4 (C2), 139.5 (C4), 130.5 (C1), 127.7 (C6), 126.7 (C3), 121.4 (C5), 47.9 (C8).

LC-MS, eluted at: 3.52 min; M = $C_8H_6N_4O_4$; calculated: m/z 222.04; found: m/z 221.2 $[M–H]^-$.

3,3-Dimethyl-2-methyleneindoline-5-carboxylic acid (5)[18,36]. 4-Hydrazinobenzoic acid (**2**) (2.00 g, 13.1 mmol, 1 eq.) was suspended in anhydrous ethanol (10 ml). 2-Methyl-2-butanone (**3**) (1.56 ml, 14.6 mmol, 1.1 eq.) and concentrated sulphuric acid (0.4 ml) were added. The mixture was stirred under reflux and N_2 for 18 h. After cooling to room temperature, the precipitate was removed by filtration and washed with acetonitrile. The filtrate was neutralised with saturated $NaHCO_3$ and washed with DCM (2×30 ml). The aqueous layer was acidified to pH 4 with 2 M HCl. The red product was extracted with DCM (3×60 ml), dried with Na_2SO_4 and the solvent was removed under vacuum to give (**5**) as a dark red solid, which was used without further purification.

^{1}H NMR (400 MHz, DMSO-d_6): δ = 12.74 (s, OH, 1H), 7.99 (d, J = 1.7, 0.6 Hz, CH–Ar (C4), 1H), 7.91 (dd, J = 7.9, J = 1.7 Hz, CH–Ar (C6), 1H), 7.50 (d, J = 8.1 Hz, CH–Ar (C7), 1H), 2.25 (s, CH_3 (C11), 3H), 1.28 (s, $2 \times CH_3$ (C12, C12), 6H).

^{13}C NMR (400 MHz, DMSO-d_6): δ = 191.7 (C2), 167.5 (C10), 157.4 (C8), 146.1 (C9), 129.6 (C6), 127.3 (C5), 122.7 (C4), 119.1 (C7), 53.5 (C3), 22.3 (C12, 13), 15.4 (C11).

LC-MS, eluted at: 2.24 min; M = $C_{12}H_{15}NO_2$; calculated: m/z 205.11; found m/z = 204.0 $[M–H]^-$.

1,3,3-Trimethyl-2-methyleneindoline-5-carboxylic acid (6)[18,36]. 3,3-Dimethyl-2-methyleneindoline-5-carboxylic acid (**5**) (1.1 g, 5.4 mmol, 1 eq.) was dissolved in a solution of anhydrous toluene : acetonitrile (2 : 1, 30 ml). To this, iodomethane (0.34 mL, 5.4 mmol, 1 eq.) was added dropwise and the solution

was refluxed at 95 °C for 24 h. The solution was cooled to room temperature and the red precipitate was collected by filtration, washed with ethanol (5 ml) and hexane (30 ml) and then dried under vacuum for 4 h to give (**6**) as a light pink solid.

^{1}H NMR (400 MHz, DMSO-d_6): δ = 8.38 (s, Ar–H (C4), 1H), 8.19 (d, J = 9.7 Hz, Ar–H (C6), 1H), 8.02 (d, J = 8.6 Hz, Ar–H (C7), 1H), 3.99 (s, CH_3 (C11), 3H), 2.80 (s, CH_3 (C12), 3H), 1.56 (s, 2 × CH_3 (C13, C14), 6H). Unassigned peaks: unreacted starting material, other impurities.

^{13}C NMR (400 MHz, DMSO-d_6): δ = 199.0 (C2), 166.5 (C10), 145.2 (C9), 142.0 (C8), 137.3 (C5), 131.6, 130.4, 128.9, 128.2, 125.3, 124.2, 115.3 (C4, C5, C6, C7, unreacted starting material and other impurities), 54.2 (C3), 34.9 (C11), 21.5 (C13, C14), 21.04 (unreacted starting material), 14.4 (C12).

LC-MS, eluted at: 0.43 min; M = $C_{13}H_{16}NO_2^+$; calculated: m/z 218.12; found: m/z 218.1 $[M]^+$.

8-(Azidomethyl)-1′,3′,3′-trimethyl-6-nitrospiro[chromene-2,2′-indoline]-5′-carboxylic acid (7). 3-Azidomethyl-2-hydroxy-5-nitrobenzaldehyde (**4**) (30 mg, 0.1 mmol, 1 eq.) and 5-carboxy-1,2,3,3-tetramethyl-3*H*-indoliumiodide (**6**) (46 mg, 0.1 mmol, 1 eq.) were added to a microwave vial (5 ml) equipped with a stirrer bar. Dry acetonitrile (3 ml) was added to the vial, followed by triethylamine (18.42 μl). The reaction was microwaved at 40 °C for 10 minutes at 250 W. The reaction was cooled to room temperature and a yellow/brown solid was collected and washed with acetonitrile (5 ml). The compound was dried under vacuum to yield a dark yellow solid.

^{1}H NMR (400 MHz, DMSO-d_6): δ 12.35 (s, OH, 1H), 8.27 (d, J = 2.8 Hz, Ar–H (C5), 1H), 8.17 (d, J = 2.8 Hz, Ar–H (C7), 1H), 7.81 (dd, J = 8.2, 1.7 Hz, Ar–H (C6′), 1H), 7.69 (d, J = 1.8 Hz, Ar–H (C4′), 1H), 7.29 (t, J = 10.5 Hz, (C4), 1H), 6.70 (d, J = 8.3 Hz, Ar–H (C7′), 1H), 6.06 (d, J = 10.4 Hz, Ar–H (C3), 1H), 4.34 – 4.21 (m, CH_2–N_3 (C11), 2H), 2.76 (s, CH_3 (C13′), 3H), 1.27 & 1.16 (s, 2 × CH_3 (C11′, C12′), 6H).

^{13}C NMR (400 MHz, DMSO-d_6): δ 167.4 (C10′), 156.8 (C9), 151.0 (C8′), 140.1 (C9′), 135.7 (C6), 130.8 (C6′), 128.4 (C4), 125.7 (C7), 122.9 (C4′, C5), 122.7 (C5′), 121.7 (C3), 120.9 (C8), 118.9 (C10), 106.5 (C7′), 106.3 (C2), 51.4 (C3′), 48.0 (C11), 28.32 (C13′), 25.6 & 19.5 (C11′, C12′).

LC-MS, eluted at: 2.35 min; M = $C_{21}H_{19}N_5O_5$; calculated: m/z 420.13; found: m/z 420.0 $[M]^-$.

Spiropyran activity

Fluorescence spectroscopy. Fluorescence spectra were recorded with a Varian Cary Eclipse Fluorescence spectrophotometer. Emission spectra were recorded with λ_{Ex} = 350 nm and λ_{Ex} = 550 nm to detect the spiropyran and merocyanine signals, respectively. Measurements were performed in either water, acetonitrile/water (1 : 1 vol%) or indicator-free neurobasal media. For each solvent system, the instrument was baseline corrected for that solvent. The spiropyran derivative **7** was first pre-conditioned by keeping it in the dark for 1 h. It was then exposed either to sunlight or UV light (365 nm, 8 W) for 15 min.

Silica nanoparticle (SiNP) synthesis and surface modification. The Stöber method was used to synthesise silica nanoparticles (SiNPs) following literature procedures.[37] NH_4OH (500 μl) was added to ethanol (16.75 ml) and stirred for 15 min. Triethoxyorthosilicate (500 μl, 0.0012 mmol) was added dropwise. This solution was left to stir for 24 h. The resulting particles were used without further purification for the subsequent surface modification process. The size and shape of the nanoparticles were characterized by TEM and DLS.

Surface modification of SiNPs with dopamine. The SiNP functionalisation with dopamine followed the steps outlined in Fig. S7 (SI) using previously reported methods.[38] Amine groups are introduced on the particle surface by adding 1 ml of a 0.1% solution of (3-aminopropyl)trimethoxysilane (APTMS) (4.2 μmol) in toluene to a suspension of SiNPs. The mixture was stirred overnight. Amine modified SiNPs were isolated and purified by centrifugation/redispersion at 12 000 rpm for 20 min. To introduce carboxylic acid functionalities on the particle surface, purified particles were redispersed in 5 ml of a 0.1 mM (0.5 μmol) succinic anhydride solution in DMF,[20] left to stir under N_2 for 24 h. The resulting carboxylic acid terminated nanoparticles were purified as described above. To attach dopamine to the carboxylic acid functionalised particles, 5 ml of a 40 mM solution of dopamine hydrochloride (0.2 mmol, 1 eq.) in dry DMF was added to the particles. To this suspension, *N*,*N*′-diisopropylcarbodiimide (2 eq.) and triethylamine (1 eq.) were added. Nanoparticles were stirred under N_2 overnight. Dopamine-modified nanoparticles were washed with ethanol by centrifugation/redispersion at 12 000 rpm for 20 min and then redispersed in neurobasal indicator-free cell culture media containing 1 mM glutathione to prevent dopamine oxidation.[39]

Surface modification of SiNPs with spiropyran–dopamine (SiNP–SP–DA). The procedure to prepare SiNP–SP–DA is illustrated in Fig. S6 (SI) and Fig. 3A. Amine-modified SiNPs were redispersed in 5 ml of a 20 mM solution of 4-pentynoic acid. To this suspension, *N*,*N*′-diisopropylcarbodiimide (2 eq.) was added. The mixture was left to stir overnight. The resulting alkyne terminated nanoparticles were purified as described above and redispersed in 5 ml of a 20 mM solution of compound **7** (0.1 mmol, 1 eq.) in DMSO:H_2O (2 : 1). To this suspension, copper sulfate (0.1 eq.) and sodium ascorbate (0.5 eq.) were added under N_2. The suspension was left to stir overnight. Subsequently, purified spiropyran-modified nanoparticles were redispersed in 5 ml of a 40 mM solution of dopamine (0.2 mmol, 1 eq.) in dry DMF. To this solution, *N*,*N*′-diisopropylcarbodiimide (2 eq.) and triethylamine (1 eq.) were added. Nanoparticles were stirred under N_2 overnight. Spiropyran–dopamine modified nanoparticles (SiNP–SP–DA) were washed with ethanol by centrifugation/redispersion at 12 000 rpm for 20 min, then redispersed in neurobasal indicator-free cell culture medium containing 1 mM of glutathione. The surface modification was followed by zeta potential measurements and FTIR spectroscopy.

Particle characterisation

Dynamic light scattering (DLS) and zeta potential measurements were performed on a Zetasizer Nano ZS (Malvern Instrument Ltd) equipped with a 5 mW He–Ne-laser source (633 nm) in a non-invasive backscattering configuration (detection angle of 173° with respect to the incident laser light) at 25 °C. For the

measurements, particle stock solutions were diluted in ethanol to give concentrations of 100 μl stock per ml ethanol.

Transmission electron microscopy (TEM) was conducted on a FEI Technai 12, Biotwin. A drop of silica nanoparticles in ethanol (1 mg ml^{-1}) was deposited onto Formvar-coated Cu grids (EM Resolutions Ltd, United Kingdom). The suspension was allowed to settle on the grid for 24 h. The median diameter and size distribution of the silica particles were determined using built in functions in ImageJ (ImageJ 1.5i) software.

FTIR-ATR spectroscopy was conducted using an Agilent Cary 63. Spectra were background corrected. Data was acquired with a resolution of 16 cm^{-1}, using 254 scans per sample.

In vitro pharmacology

SH-SY5Y cell culture and activation assay in the presence of modified particles. SH-SY5Y cells (ATCC®, CRL-2266TM) were cultured in DMEM medium supplemented with 5% penicillin/streptomycin, 5% glutamine and 10% heat-inactivated fetal bovine serum (FBS), Gibco, Life Technologies, Frederick, MD in an atmosphere of 5% CO_2 at 37 °C. Cells were differentiated into mature neuronal cells using retinoic acid as described previously.[40] Cells were cultured for 24 h as described above. Then, the medium was changed to serum free differentiation medium (ATRA-containing neurobasal medium) to promote differentiation and the neuronal phenotype. Cells were cultured for 5 days, refreshing the medium every 48 h. Differentiation was confirmed by microscopy *via* morphological assessment of neurite outgrowth.

Mature neuronal cells were treated with 1 mM MPP+ for 24 h.[32] Then the cells were left to rest for one day before adding the different SiNPs. SiNPs were either incubated under UV or white light for 30 min prior to the treatment to either activate (open merocyanine form, SiNP–MC–DA) or deactivate (closed spiropyran form, SiNP–SP–DA) the compound. Cells were treated with 62.5 μg ml^{-1} of modified SiNPs for either 30 min or 60 min. After exposure to the particles, a cAMP-Glo (Promega#V1502) assay was performed according to the manufacturer's instructions.

CRE/DRD1 transfection and one glow assay in the presence of modified particles. HEK293 cells were cultured in cell culture medium (DMEM medium) supplemented with 1% penicillin/streptomycin, 1% AB/AM, 1% glutamine and 10% heat-inactivated fetal bovine serum (FBS), in an atmosphere of 5% CO_2 at 37 °C. After 48 h, the cells were subcultured using 50 000 cells per well into 48 well plates for transfection. Cells were incubated for 24 h. Then the DMEM medium was replaced with 100 μl of transfection medium.

Transfection medium preparation. To a sterile tube, 88 μl serum free medium, prewarmed to room temperature, was added. Then, 2 μl of CRE plasmid DNA (1 μg μl^{-1}) pGL4.29-[luc2P/CRE/Hygro] Vector (Promega Cat: E8471) and 2 μl DRD1 DNA were added and mixed by pipetting. Subsequently, 8 μl FuGENER 4K Transfection Reagent (Promega Cat: E5911) was added and mixed. The resulting solution was applied immediately to the cells in a drop-wise manner. Cells were then incubated for 24–72 h.

MTT cytotoxicity assay in the presence of unmodified SiNPs. SH-SY5Y and CRE/DRD1 transfected HEK293 cells were cultured in the presence of SiNPs for 24 h using the same cell culture protocols described above. SiNP concentrations of 15 μg ml^{-1}, 31.25 μg ml^{-1}, 62.5 μg ml^{-1}, 125 μg ml^{-1}, 250 μg ml^{-1}, 500 μg ml^{-1} and 1000 μg ml^{-1} were used. Cells cultured without SiNPs were used as controls. Cell viability was measured with an Invitrogen™ CyQUANT™ MTT Cell Viability Assay (Catalogue number: V13154) following the manufacturers' instructions.

Dopamine–spiropyran modified silica nanoparticle treatment. Transfected cells were treated with 62.5 μg ml^{-1} of modified SiNPs. Luciferase activity was measured after 30 min, 60 min and 120 min using the One-Glo™ Luciferase Assay System (Promega, cat, E6110); 100 μl of the assay mix was added to the cells in the well, followed by measuring the luminescence.

Docking study

Selection and optimisation of target receptors. The crystal structure of D_1R (PDB ID:7CKW)[35] was used to perform docking studies with the open and closed forms of the dopamine–spiropyran conjugates. The 3D structures were prepared with UCSF Chimera, removing water molecules and other non-protein ligands. As ligands for the docking study, we used dopamine and the merocyanine and spiropyran form of the spiropyran–dopamine conjugates. The latter included a triazole moiety to mimic the attachment site to the remainder of the SiNPs (Fig. 5A and B). The 3D structures of dopamine were downloaded from the PubChem database in '.mol2' format. The other compounds were drawn and imported from ChemDraw.

Docking study. Docking was performed using AutoDock Vina 9. The docking site was selected upon the location of the co-crystalized ligands. For each docking, a grid box of *x* 33, *y* 33, and *z* 33 Å was chosen. Discovery studio visualiser was used to illustrate the 2D structure of the ligand–receptor interaction.

Author contributions

Conceptualization, M.Z. (Mischa Zelzer), H.G. (Hajar Alghamdi) and N.A.R. (Noah A. Russell); methodology, M.Z., H.G., S.N.M. (Shailesh N. Mistry), S.R. (Sunil Rajput); software, H.G.; validation, H.G.; formal analysis, H.G.; investigation, H.G.; resources, H.G., M.Z.; data curation, H.G.; writing – original draft preparation, H.G.; writing – review and editing, H.G., M.Z.; G.M. (Giuseppe Mantovani), S.N.M., P.G. (Pavel Gershkovich), K.S. (Keith Spriggs), C.A.L. (Charles A. Laughton); visualization, H.G., M.Z.; supervision, M.Z., C.L., G.M., P.G., K.S.; project administration, M.Z.; funding acquisition, H.G., M.Z., N.A.R. All authors have read and agreed to the published version of the manuscript.

Conflicts of interest

There are no conflicts to declare.

Data availability

Raw and processed data for this article are available from Nottingham Research Data Management Repository *via* the following link: DOI: https://doi.org/10.17639/nott.7619.

The data include processed NMR spectra, raw fluorescence and infrared spectroscopy data and the TEM image.

Supplementary information (SI): NMR spectra, nanoparticle surface modification procedure and additional characterisation data, control experiments for receptor activation and molecular docking of dopamine in the D_1R. See DOI: https://doi.org/10.1039/d6ma00037a.

Acknowledgements

This work was financially supported by the Saudi Ministry of education *via* University of Hafr Albatin. Parts of Fig. 1 and 3 were created in BioRender. Alghamdi, H. (2026).

Notes and references

1 D. W. Dickson, *Parkinsonism Relat. Disord.*, 2018, **46**, S30–S33.
2 Y. Luo, L. Qiao, M. Li, X. Wen, W. Zhang and X. Li, *Front. Aging Neurosci.*, 2025, **16**(2024), 16:1498756.
3 D. Su, Y. Cui, C. He, P. Yin, R. Bai, J. Zhu, J. S. T. Lam, J. Zhang, R. Yan, X. Zheng, J. Wu, D. Zhao, A. Wang, M. Zhou and T. Feng, *BMJ*, 2025, **388**, e080952.
4 A. Wijers, A. Ravi, S. M. A. A. Evers, G. Tissingh and G. A. P. G. van Mastrigt, *Mov. Disord*, 2024, **39**, 1938–1951.
5 T. Foltynie, V. Bruno, S. Fox, A. A. Kühn, F. Lindop and A. J. Lees, *Lancet*, 2024, **403**, 305–324.
6 P. A. LeWitt, *N. Engl. J. Med.*, 2008, **359**, 2468–2476.
7 S. Hisahara and S. Shimohama, *Int. J. Med. Chem.*, 2011, **2011**, 403039.
8 T. Mestre and J. J. Ferreira, *Ther. Adv. Neurol. Disord.*, 2010, **3**, 117–126.
9 P. Yang, F. Zhu, Z. Zhang, Y. Cheng, Z. Wang and Y. Li, *Chem. Soc. Rev.*, 2021, **50**, 8319–8343.
10 J. Shi, C. Tan, X. Ge, Z. Qin and H. Xiong, *J. Mater. Chem. B*, 2024, **12**, 5769–5786.
11 A. Raza, T. Rasheed, F. Nabeel, U. Hayat, M. Bilal and H. M. N. Iqbal, *Molecules*, 2019, **24**, 1117.
12 B. E. Hetzler, P. Donthamsetti, R. M. Wolesensky, C. Stanley, E. Y. Isacoff and D. Trauner, *ACS Chem. Biol.*, 2025, **20**, 2609–2616.
13 P. C. Donthamsetti, N. Winter, M. Schönberger, J. Levitz, C. Stanley, J. A. Javitch, E. Y. Isacoff and D. Trauner, *J. Am. Chem. Soc.*, 2017, **139**, 18522–18535.
14 D. Lachmann, C. Studte, B. Männel, H. Hübner, P. Gmeiner and B. König, *Chem. - Eur. J.*, 2017, **23**, 13423–13434.
15 C. Matera, P. Calvé, V. Casadó-Anguera, R. Sortino, A. M. J. Gomila, E. Moreno, T. Gener, C. Delgado-Sallent, P. Nebot, D. Costazza, S. Conde-Berriozabal, M. Masana, J. Hernando, V. Casadó, M. V. Puig and P. Gorostiza, *Int. J. Mol. Sci.*, 2022, **23**, 10114.
16 R. Klajn, *Chem. Soc. Rev.*, 2014, **43**, 148–184.
17 L. Kortekaas and W. R. Browne, *Chem. Soc. Rev.*, 2019, **48**, 3406–3424.
18 X. Z. Zhang, S. Heng and A. D. Abell, *Chem. - Eur. J.*, 2015, **21**, 10703–10713.
19 W. G. Tian and J. T. Tian, *Dyes Pigm.*, 2014, **105**, 66–74.
20 Y. An, M. Chen, Q. Xue and W. Liu, *J. Colloid Interface Sci.*, 2007, **311**, 507–513.
21 Y. Q. Xu, L. Y. Xiao, Y. T. Chang, Y. A. Cao, C. G. Chen and D. Wang, *Materials*, 2020, **13**, 1279.
22 B. Liao, P. Long, B. Q. He, S. J. Yi, B. L. Ou, S. H. Shen and J. Chen, *J. Mater. Chem. C*, 2013, **1**, 3716–3721.
23 R. D. Macuil, M. R. Lopez, A. O. Díaz and V. C. Pernas, presented in part at the J. Phys.: Conf. Ser., 2009.
24 A. Thakur, S. Ranote, D. Kumar, K. K. Bhardwaj, R. Gupta and G. S. Chauhan, *ACS Omega*, 2018, **3**, 7925–7933.
25 J. L. Biedler, S. Rofflertarlov, M. Schachner and L. S. Freedman, *Cancer Res.*, 1978, **38**, 3751–3757.
26 26S. Pahlman, A. I. Ruusala, L. Abrahamsson, M. E. K. Mattsson and T. Esscher, *Cell Differ.*, 1984, **14**, 135–144.
27 Y. T. Cheung, W. K. W. Lau, M. S. Yu, C. S. W. Lai, S. C. Yeung, K. F. So and R. C. C. Chang, *Neurotoxicology*, 2009, **30**, 127–135.
28 K. M. Pettifer, S. C. Jiang, C. Bau, P. Ballerini, I. D'Alimonte, E. S. Werstiuk and M. P. Rathbone, *Purinergic Signalling*, 2007, **3**, 399–409.
29 K. J. Bell, T. I. Lansakara, R. Crawford, T. B. Monroe, A. V. Tivanski, A. K. Salem and L. L. Stevens, *Toxicol. In Vitro*, 2021, **70**, 105031.
30 A. Lees, E. Tolosa, F. Stocchi, J. J. Ferreira, O. Rascol, A. Antonini and W. Poewe, *Expert Rev. Neurother.*, 2023, **23**, 15–24.
31 G. A. Keller, P. Czerniuk, R. Bertuola, J. G. Spatz, A. R. Assefi and G. Di Girolamo, *Clin. Ther.*, 2011, **33**, 500–510.
32 Y. J. Jung, H. Choi and E. Oh, *Neurosci. Lett.*, 2021, **765**, 136265.
33 F. Wang, F. Gao, M. Lan, H. Yuan, Y. Huang and J. Liu, *Toxicol. In Vitro*, 2009, **23**, 808–815.
34 H. Yuan, F. Gao, Z. Zhang, L. Miao, R. Yu, H. Zhao and M. Lan, *J. Health Sci.*, 2010, **56**, 632–640.
35 P. Xiao, W. Yan, L. Gou, Y.-N. Zhong, L. Kong, C. Wu, X. Wen, Y. Yuan, S. Cao, C. Qu, X. Yang, C.-C. Yang, A. Xia, Z. Hu, Q. Zhang, Y.-H. He, D.-L. Zhang, C. Zhang, G.-H. Hou, H. Liu, L. Zhu, P. Fu, S. Yang, D. M. Rosenbaum, J.-P. Sun, Y. Du, L. Zhang, X. Yu and Z. Shao, *Cell*, 2021, **184**(4), 943–956.e18.
36 D. B. Stubing, S. Heng and A. D. Abell, *Org. Biomol. Chem.*, 2016, **14**, 3752–3757.
37 W. Stober, A. Fink and E. Bohn, *J. Colloid Interface Sci.*, 1968, **26**, 62–69.
38 H. S. Jung, D. S. Moon and J. K. Lee, *J. Nanomater.*, 2012, **2012**, 593471.
39 D. Rana, T. Colombani, H. S. Mohammed, L. J. Eggermont, S. Johnson, N. Annabi and S. A. Bencherif, *Emergent Mater.*, 2019, **2**, 209–217.
40 J. Kovalevich, M. Santerre and D. Langford, Neuronal Cell Culture, in *Methods And Protocols*, ed. S. Amini and M. K. White, 2nd edn, 2021, vol. 2311, pp. 9–23.